Environment International 157 (2021) 106829

Contents lists available at ScienceDirect

Environment International

journal homepage: www.elsevier.com/locate/envint

Metabolism of chiral sulfonate compound 2,3-dihydroxypropane-1-sulfonate (DHPS) by *Roseobacter* bacteria in marine environment

Xiaofeng Chen [a], Le Liu [a], Xiang Gao [b], Xi Dai [a], Yu Han [a], Quanrui Chen [a], Kai Tang [a,*]

[a] State Key Laboratory of Marine Environmental Science, College of Ocean and Earth Science, Xiamen University, Xiamen 361102, Fujian, PR China
[b] School of Pharmaceutical Sciences, Fujian Provincial Key Laboratory of Innovative Drug Target Research, Xiamen University, Xiamen 361102, Fujian, PR China

ARTICLE INFO

Handling Editor: Adrian Covaci

Keywords:
Sulfonates
Ocean
Bacteria
Proteomic
Roseobacter
Chirality

ABSTRACT

The sulfonate compound 2,3-dihydroxypropane-1-sulfonate (DHPS) is one of the most abundant organic sulfur compounds in the biosphere. DHPS derived from dietary intake could be transformed into sulfide by intestinal microbiota and thus impacts human health. However, little is known about its sulfur transformation and subsequent impacts in marine environment. In this study, laboratory-culturing was combined with targeted metabolomic, chemical fluorescence probing, and comparative proteomic methods to examine the bioavailability of chiral DHPS (R and S isomers) for bacteria belonging to the marine *Roseobacter* clade. The metabolic potential of DHPS in bacteria was further assessed based on genomic analysis. *Roseobacter* members *Ruegeria pomeroyi* DSS-3, *Dinoroseobacter shibae* DFL 12, and *Roseobacter denitrificans* OCh 114 could utilize chiral DHPS for growth, producing sulfite. They all contained a similar gene cluster for DHPS metabolism but differed in the genes encoding enzymes for desulfonation. There was no significant difference in the growth rate and DHPS consumption rate for *R. pomeroyi* DSS-3 between R- and S-DHPS cultures, with few proteins expressed differentially were found. Proteomic data suggested that a series of hydrogenases oxidized DHPS, after which desulfonation could proceed via three distinct enzymatic pathways. Strain *R. pomeroyi* DSS-3 completed the desulfonation via L-cysteate sulfo-lyase, while *D. shibae* DFL 12 and *R. denitrificans* OCh 114 primarily utilized sulfolactate sulfo-lyase, and sulfopyruvate decarboxylase followed by sulfoacetaldehyde acetyltransferase, respectively, to complete desulfonation releasing the sulfonate-moiety. The sulfite could be further oxidized or incorporated into sulfate assimilation, indicated by the proteomic data. Furthermore, DHPS metabolic pathways were found primarily in marine bacterial groups, including the majority of sequenced *Roseobacter* genomes. Our results suggest that chiral DHPS, as a vital reduced sulfur reservoir, could be metabolized by marine bacteria, providing a resource for bacterial growth, rather than acting as a source of toxic sulfide within the marine ecosystem.

1. Introduction

Biogenic sulfur metabolites constitute the major component of the upper ocean dissolved organic sulfur (DOS) pool (Moran and Durham, 2019), and are primarily composed of sulfur-containing amino acids and their derivatives, methyl-sulfur compounds, sulfonates, and sulfate esters (Moran and Durham, 2019; Tang, 2020). These molecules could be efficiently scavenged by bacteria, but, with the exception of the methyl-sulfur compound dimethylsulfoniopropionate (DMSP) (Moran and Durham, 2019), little is known about the transformation process and metabolic fate of DOS molecules. Recently, sulfonates, which act as ecologically important currencies in trophic interactions, have been of increasing interest (Durham et al., 2017; Durham et al., 2019; Landa et al., 2019; Moran and Durham, 2019). Among them, 2,3-dihydroxypropane-1-sulfonate (DHPS), is especially important due to its widespread abundance. DHPS can be derived from the microbial degradation of sulfoquinovose (Denger et al., 2014), a ubiquitous compound in photosynthetic organisms with an estimated annual global production of 10^{10} tons (Harwood and Nicholls, 1979). DHPS is also a major constituent of the cytoplast component in marine phytoplankton, especially within diatoms and coccolithophores (Durham et al., 2015; 2019). Marine diatoms, which contribute an estimated ~40% of the global marine primary production (Nelson et al., 1995), harbor high millimolar intercellular concentrations of DHPS that are comparable to that of DMSP (Durham et al., 2015). DHPS could be released into the DOS pool via various processes (such as exudation, senescence and cell lysis),

* Corresponding author.
E-mail address: tangkai@xmu.edu.cn (K. Tang).

https://doi.org/10.1016/j.envint.2021.106829
Received 31 December 2020; Received in revised form 12 August 2021; Accepted 13 August 2021

which has been found in seawater during diatom blooms (Durham et al., 2015), and thus would be available for marine heterotrophic bacteria (Durham et al., 2017; Moran and Durham, 2019). Moreover, meta-transcriptomic and meta-metabolomic analyses have suggested that a sulfonate-based metabolic network, including DHPS, presents between phytoplankton and bacteria in the North Pacific (Durham et al., 2019).

With the rising incidence of inflammatory bowel diseases (Ng et al., 2017), there has been an increasing concern that dietary DHPS could be converted by intestinal microbiota into sulfide (Liu et al., 2020), which could serve as a pathogeny of intestinal inflammation and colorectal cancer (Carbonero et al., 2012). Sulfide is toxic to most marine organisms due to the inhibition of aerobic respiration(Sohn et al., 2000), and therefore has negative impacts on the marine ecosystem. The consequence of DHPS metabolism in the marine environment remains unknown. Moreover, it should be noted that chirality is common among sulfonates and that chiral selectivity may exist among enzymes catalyzing these compounds. The ubiquitous L-amino acids have been demonstrated to be much more labile than their respective isomers (Wang et al., 2020). According to previous studies, S-DHPS could be transformed to R-DHPS, that in turn could be oxidized to 3-sulfolactate by dehydrogenase, which is then further catabolized (Mayer et al., 2010), indicating a potential difference of biotransformation process between R- and S-DHPS. However, experimental evidence is lacking.

The ubiquitous marine bacterioplankton, *Roseobacter* clade, is considered as important mediator of sulfur flux in the upper ocean with respect to the transformation and mineralization of organic sulfur compounds (Landa et al., 2019). In this study, laboratory incubations combined with physiological, targeted metabolomic, and proteomic methods were used to examine the bioavailability of R-DHPS and S-DHPS for bacteria belonging to the marine *Roseobacter* clade and to investigate the enzymatic pathways involved. A chemical fluorescence probe CY, which is superior to conventional analytical techniques (Nie et al., 2020), was used for the real time monitoring of sulfur transformation of DHPS. Furthermore, we analyzed the genetic capability of bacterial DHPS catabolism based upon sequenced genomes. This work would further improve our understanding of DHPS metabolism and its potential impact on marine ecosystem.

2. Materials and methods

2.1. Chemical synthesis of R -DHPS and S-DHPS.

To obtain R-DHPS, sodium sulfite (1.2 g, 9.24 mmol) was dissolved in water (10 ml), to which R-3-chloro-1,2-propanediol (1.072 g, 9.70 mmol) was added. The solution was refluxed by heating for 2 h. After completion of the reaction, the solution was concentrated, and methanol (10 ml) was added to the concentrated residue. Crystals that formed were filtered, and the resulting crystalline solids were dried to obtain the product (2.026 g, yield 82.7%) as white and more powdery crystals. Similarly, the pure enantiomer S-DHPS was obtained analogously from S-3-chloro-1,2-propanediol. The chemical structures of R-DHPS and S-DHPS were identified by using ^{1}H and ^{13}C NMR (Fig. S1), and MS/MS (Fig. S2).

R-DHPS: ^{1}H NMR (600 MHz, D_2O): δ = 4.10(m, 1H)3.65, (dd, J = 11.76, 3.96 Hz, 1H), 3.54(dd, J = 12.0, 6.36 Hz, 1H) 0.3.07(dd, J = 14.49, 4.32 Hz, 1H)2.99(dd, J = 14.46, 7.62 Hz, 1H)ppm. ^{13}C NMR (151 MHz, D_2O): δ = 68.1(CH_2)64.6(H)53.7(CH_2)ppm. $[\alpha]_D^{24} = -6.700$ (c 0.064, H_2O). ESI-MS: m/z = ([M−H]$^-$, theoretical mass: 155.0020, relative error: ppm).

S-DHPS: ^{1}H NMR (600 MHz, D_2O): δ = 4.11(m, 1H),3.66(dd, J = 11.82, 3.96 Hz, 1H),3.55(dd, J = 11.82, 6.36 Hz, 1H),3.08(dd, J = 14.46, 4.26 Hz, 1H),2.99 (dd, J = 14.46, 7.68 Hz, 1H)ppm. ^{13}C NMR (151 MHz, D_2O): δ68.1(CH_2),64.6(CH),53.7(CH_2)ppm. $[\alpha]_D^{24} = +4.570$ (c 0.064, H_2O). ESI-MS: m/z = ([M−H]$^-$, theoretical mass: 155.0020, relative error: ppm).

2.2. Organisms and growth media

All glassware was acid-cleaned. The *Roseobacter* strains *Ruegeria pomeroyi* DSS-3 (DSM 15171) (Gonzalez et al., 2003), *Dinoroseobacter shibae* DFL 12 (DSM 16493) (Biebl et al., 2005), *Roseobacter denitrificans* OCh 114 (DSM 7001) (Shiba, 1991), and *Nautella italica* DSM 26436 (Vandecandelaere et al., 2009) were obtained from the German Culture Collection (DSMZ, Braunschweig, Germany). Triplicate pure cultures were incubated at 28 °C in modified *Silicibacter* basal medium (Denger et al., 2006), pH 7.2. A supplement of yeast extract (0.025%) was required by strains *R. denitrificans* OCh 114, *D. shibae* DFL 12, and *N. italica* DSM 26436. Either 10 mM DHPS or 15 mM acetate was added to the appropriate medium. 10 mM ammonium chloride was used as the nitrogen source. To transfer cultures to basal medium, strains were pre-grown in 2216E liquid medium (Hopebio, China) and cells collected by centrifugation (4,000 rpm for 10 min), washed three times with sterile basal medium (without extra carbon source) and resuspended, then diluted 50-fold in the appropriate medium. All strains were grown aerobically on a shaker at 160 rpm. Samples were taken at intervals, as determined by growth through optical density measurement (OD_{600}), to determine the concentrations of DHPS and sulfite. Triplicate cell-free extracts (1 ml) for targeted metabolomics analysis were created by filtering through a 0.2 μm hydrophilic polyvinylidene fluoride (PVDF) membrane filter (13 mm, JINTENG, China) and stored at −80 °C until extraction. For proteomic analysis, triplicate cultures were conducted with different carbon sources, and cells were harvested by centrifugation at 4500 rpm and 4 °C for 20 min. Cells grown with either R-DHPS, S-DHPS or acetate were harvested at exponential phase, while those grown with mixed DHPS (R-DHPS: S-DHPS, 1:1) were harvest at both the exponential and stationary phases. The cells were washed twice with phosphate-buffered saline (PBS, pH 7.4), then were flash-frozen in liquid nitrogen and stored at − 80 °C.

2.3. Extraction and detection of DHPS

To ensure that bacterial degradation of DHPS occurred, we used targeted metabolic analysis to monitor the DHPS concentrations remaining in the supernatant. Acetonitrile: methanol: water (40:40:20, 4 °C) was used to extract extracellular DHPS. Samples were vortexed for 30 s, followed by incubation at −20 °C for 2 h, and centrifugation at 12,000 rpm for 15 min (4 °C). The clear supernatant was transferred into an autosampler vial for ultra-high performance liquid chromatography (UHPLC)-MS/MS analysis.

The concentration of DHPS was detected by an Agilent 1290 Infinity II series UHPLC system (Agilent Technologies, USA) coupled to an Agilent 6460 triple quadrupole mass spectrometer (Agilent Technologies, USA) via an AJS electrospray ionization (AJS-ESI) interface. Compound separation was achieved on a Waters ACQUITY UPLC BEH Amide column (100 × 2.1 mm, 1.7 μm), heated to 35 °C. The total eluent flow was 0.4 ml/min with 10 mM ammonium formic acid (LC-MS, CNW Technologies) and 10 mM ammonia (LC-MS, CNW Technologies) as eluent A and acetonitrile (LC-MS, CNW Technologies) as eluent B. The elution gradient was as follows: 0–5 min, B 75%; 5–7 min, B 70%; 7–8.7 min, B 50%; 8.7–14 min, B 75%. A calibration curve for standard DHPS was used to determine DHPS concentrations. The auto-sampler temperature was set at 4 °C and the injection volume was 1 μl. The parameters of operating source conditions were as follows: capillary voltage = +4000/−3500 V, Nozzle Voltage = +500/−500 V, gas (N_2) temperature = 300 °C, gas (N_2) flow = 5 L/min, sheath gas (N_2) temperature = 250 °C, sheath gas flow = 11 L/min, nebulizer = 45 psi. Agilent MassHunter Work Station Software (B.08.00, Agilent Technologies) was employed for MRM data acquisition and processing. The area ratio of DHPS (155 m/z) was plotted relative to the DHPS concentration, and the UHPLC separation pattern (Fig. S3) and its MS-MS fragmentation pattern (Fig. S2) are shown in the supplementary data.

2.4. Sulfite detection

For determination of the dynamic of sulfite concentration, the hemicyanine dyes-based fluorescent probe CY was used (Nie et al., 2020), which is able to monitor the change of sulfur dioxide derivatives (SO_3^{2-} / HSO_3^-) in seawater with a high sensitivity and stable detection (Nie et al., 2020). A stock solution of CY was prepared in PBS aqueous buffer (pH = 7.4). Before measurements, the solution was freshly prepared by diluting the high concentration stock solution to the appropriate level (final concentration of CY in the reaction mixture, 1 μM). By itself, the solution of CY displays a yellowish color with an emission maximum at 607 nm under excitation at 410 nm, with increasing sulfite concentration, the fluorescence intensity of the probe decreases gradually and the initial color of CY fades. Samples were added to the CY solution immediately after collected, at a 5% volume proportion, except for *R. pomeroyi* DSS-3 (0.5% volume proportion), then the mixtures were stirred and incubated statically at room temperature for 20 mins. 2 ml of the mixtures were then aliquoted into a 1 cm quartz cell and applied for each of the spectroscopic tests. To estimate the impact of natural oxidants and whether the bacteria present in the medium to alter sulfite concentrations, an additional experiment was done as follows: When *R. pomeroyi* DSS-3 growth entered the early stable phase (95 h), we sterilized part of the cultures filtering through a 0.2 μm filter (13 mm, Millipore, PES membrane), and then returned both the cell-free and the cell-containing cultures, back to the shaker and monitored the changes in sulfite concentration over time.

2.5. Proteomic analysis

Cells from different culture conditions, 3 biological replicates each, were harvested as described above. Sample were sonicated three times on ice using a high intensity ultrasonic processor (Scientz Biotechnology, Ningbo, China) in lysis buffer (8 M urea, 1% Protease Inhibitor Cocktail), and the cell debris were removed by centrifugation at 12,000 g at 4℃ for 10 min. Finally, the supernatant was collected and protein concentration was determined with BCA Protein Assay Kit (Beyotime, China) according to the instructions of manufacturer. The protein solution was reduced with 5 mM dithiothreitol for 30 min at 56 °C followed by cysteine alkylation with 11 mM iodoacetamide at room temperature, in the dark, for 15 min. Samples were then diluted by adding 100 mM triethylamine borane (TEAB) until the urea concentration was less than 2 M. Trypsin (Promega, Madison, WI, USA) at 1:50 (*w*/w) enzyme-protein ratio was used to digest the protein overnight, followed by a second 4 h-digestion at 1:100 (*w*/w) enzyme-protein ratio. Tryptic peptides were desalted by Strata X C18 SPE column (Phoenomenex, USA) and vacuum dried. All peptides were then resuspended in solvent A (0.1% formic acid, 2% acetonitrile), and separated using C18 column. The gradient was comprised of an increase from 6% to 22% solvent B (0.1% formic acid in 90% acetonitrile) over 40 min, 22% to 35% over 12 min, climbing to 80% in 4 min, and held at 80% for 4 min, all at a constant flowrate of 0.3 μl/min on an EASY-nLC 1000 UPLC system (Thermo Fisher Scientific). Peptides were then subjected to NSI source followed by tandem mass spectrometry (MS/MS) in Q Exactive™ Plus (Thermo Fisher Scientific) coupled online to an UPLC system. A Top20 data-dependent MS/MS scan method was used to acquire the MS data. Injection time was set to 200 ms, resolution to 60,000 at 100 *m/z*, spray voltage of 2.0 kV, and an AGC target of 5×10^4 for a full scan with a range of 350–1800 *m/z*. Precursor ions were fragmented at a normalized collision energy of 28 eV using a high-energy C-trap dissociation and the fragments were detected in the Orbitrap at a resolution of 15,000 at *m/z* 100. To avoid repeated scanning of identical peptides, we set the dynamic exclusion at 30 s. The resulting MS/MS data were processed using Maxquant search engine (v. 1.5.2.8) (Cox and Mann, 2008). Searches were performed against the genome sequences of *R. denitrificans* OCh 114, *D. shibae* DFL 12, and *R. pomeroyi* DSS-3 downloaded from the National Center for Biotechnology Information (NCBI) database (https://www.ncbi.nlm.nih.gov/), respectively. The Perseus platform (Tyanova et al., 2016) was used for bioinformatics analysis. Since each treatment was performed in triplicate, proteins identified in at least two out of the three replicates, and with at least 2 MS/MS counts were included for further analysis. Differential expression analysis was performed using LFQ intensities. After Log2 transformation of the intensities and filtering of the data, a two-tailed Fisher's exact test was used to determine differentially abundant proteins using a 1% permutation-based FDR filter. Scatter plots were used to determine the correlation between replicates. The Z-score normalized data was used to perform hierarchical clustering and to generate the heat map analysis. The Log_2FC values were used to generate heatmaps using GraphPad Prism 8.0.2 (GraphPad Software, USA).

2.6. Bioinformatic analysis

Sequenced and annotated genomes of *R. pomeroyi* DSS-3, *D. shibae* DFL 12, *R. denitrificans* OCh 114, and *N. italica* DSM 26436 were obtained from the NCBI database. To identify genes related to the metabolism of DHPS and DMSP in bacterial genomes, each protein sequence derived from the above *Roseobacter* genomes was queried using BLASTP against Uniport databases (https://www.uniprot.org) (Altschul et al., 1997), and sequences with E-value of <1e−5 and sequence identity >30% were retained. Sequences with an identity score of < 50% were further manually checked, from those with the lowest threshold to those with the highest threshold, blasting against the NCBI non-redundant protein database and checking the top matching annotation result. A phylogenetic tree of *Roseobacter* strains was constructed using RAxML (Stamatakis, 2014) with PROTGAMMAJTT and 1000 bootstrap replicates. Phylogenetic trees of bacterial 16S rRNA were constructed with MEGA 6.0 employing the neighbor-joining method (Tamura et al., 2013). The proteomic data have been deposited to the National Omics Data Encyclopedia (NODE, https://www.biosino.org/node) with the accession number OEP001337.

3. Results and discussion

3.1. DHPS metabolic genes

The predicted pathway of DHPS mineralization by bacteria, shown in Fig. 1A, can be separated into three stages: DHPS dehydrogenation, desulfonation, and sulfite oxidation. Variants of the canonical pathway for DHPS catabolism are also shown (Fig. 1B).

3.1.1. Stage 1 DHPS dehydrogenation

In *Ruegeria pomeroyi* DSS-3, *Dinoroseobacter shibae* DFL 12, and *Roseobacter denitrificans* OCh 114, the DHPS dehydrogenases genes (*hpsO*, *hpsP* and *hpsN*) are part of an apparent operon, which also contains transcriptional regulators (*hpsR* and *hpsQ*) (Fig. 1B). Dehydrogenases HpsOP are responsible for the conversion of S-DHPS into R-DHPS, which is converted by dehydrogenase HpsN into sulfolactate, then desulfonated via one of the three enzymatic pathways (Fig. 1A).

3.1.2. Stage 2 DHPS desulfonation

Key genes involved in desulfonation are not organized in the same manner within the operons of different strains (Fig. 1B). *CuyA* (encoding L-cysteate sulfo-lyase) are present in the genomes of all three strains (Fig. 1B). In *R. pomeroyi* DSS-3, sulfolactate could be dehydrogenated by sulfolactate dehydrogenases (encoded by genes *slcD* and *comC*) into 3-sulfopyruvate, which is converted to cysteate followed by C-S cleavage via L-cysteate sulfo-lyase, producing pyruvate and sulfite (Fig. 1). Apart from *cuyA*, additional genes *comDE* (encoding sulfopyruvate decarboxylase) and *xsc* (encoding sulfoacetaldehyde acetyltransferase) are present in *R. denitrificans* OCh 114, indicating that 3-sulfopyruvate could be converted via another pathway in which it is decarboxylated to sulfoacetaldehyde via sulfopyruvate decarboxylase (ComDE) followed by C–S

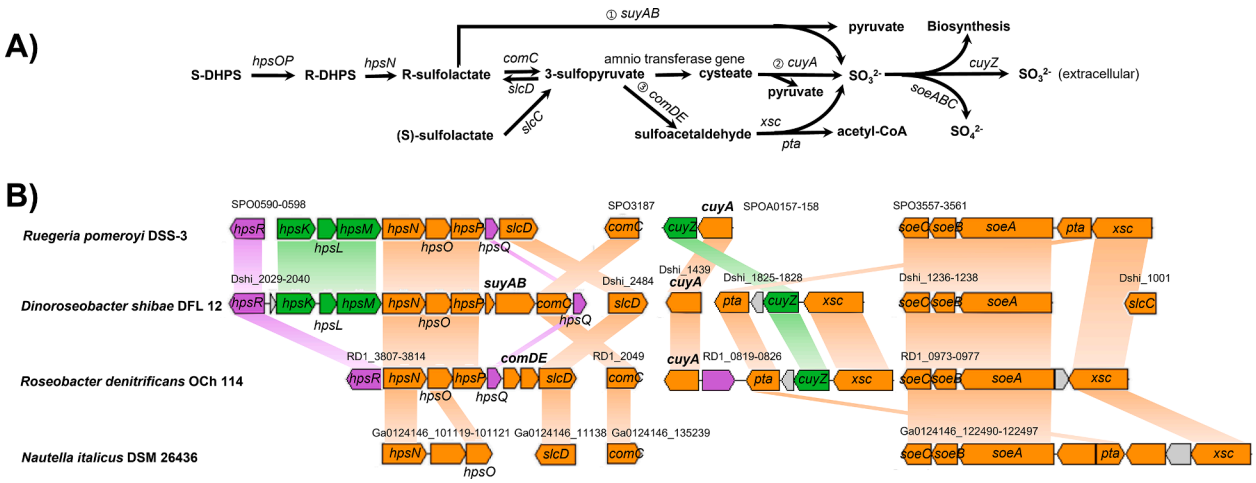

Fig. 1. The high diversity of DHPS catabolism. A) Biochemical processes involved in the transformation and biomineralization of DHPS by marine bacteria, showing all three desulfonation pathways; B) Gene clusters encoding the proteins involved in the degradation of DHPS, similar to those found in *R. pomeroyi* DSS-3, with locus tags and annotations. Protein function is color-coded: purple, transcriptional regulators and universal stress proteins; green, transporters; orange, enzymes directly involved in DHPS degradation; gray, other genes. Homologous genes are connected by colored bars between the genomes. (For interpretation of the references to colour in this figure legend, the reader is referred to the web version of this article.)

cleavage by sulfoacetaldehyde acetyltransferase (Xsc), yielding acetyl-CoA and sulfite (Fig. 1). As for *D. shibae* DFL 12, it harbors *suyAB* (encoding sulfolactate sulfo-lyase), in addition to *cuyA*, this presents the potential to directly cleave sulfolactate at the C-S bond by sulfolactate sulfo-lyase (SuyAB), producing pyruvate and sulfite (Fig. 1). The produced pyruvate or acetyl-CoA would further enter the tricarboxylic acid cycle, serving as a resource of carbon and energy for bacterial growth.

3.1.3. Stage 3 Sulfite oxidation

Though different *Roseobacter* strains may catabolize DHPS via distinct pathways, all three desulfonation pathways could produce sulfite. Sulfite-oxidizing enzyme (SoeABC), which has been known as the major detoxification mechanism for cytoplasmic sulfite from the desulfonation of sulfonates, could oxidize sulfite into sulfate and transfer the resulting electrons to the electron transport chain (Dahl et al., 2013). The four strains all harbor *soeABC* genes, indicting the potential of subsequent sulfite oxidation (Fig. 1B) for energy generation.

3.2. Growth of Roseobacter strains with DHPS

Strains *R. pomeroyi* DSS-3, *D. shibae* DFL 12, and *R. denitrificans* OCh 114, but not *N. italica* DSM 26436, could utilize DHPS for exponentially growth (Fig. S4). Bacterial growth rates of *R. pomeroyi* DSS-3 and *D. shibae* DFL 12 showed no observable differences between R- and S-DHPS incubation experiments ($p > 0.05$, *t*-test; Fig. S4). The concentrations of DHPS decreased during the incubation of strains *R. pomeroyi* DSS-3, *D. shibae* DFL 12 and *R. denitrificans* OCh 114 (Fig. 2), with < 10% of the added DHPS remaining, and no significant differences in the DHPS consumption rate ($p > 0.05$, *t*-test; Fig. 2) were found between R- and S-DHPS cultures. While that of *N. italica* DSM 26436 incubation showed negligible change (Fig. S5). The failure of *N. italica* DSM 26436 to utilize DHPS might be due to the lack of not only *hpsKLM* (encoding DHPS transporters) and *hpsP* genes, but also genes encoding key desulfonative enzymes (Fig. 1B).

3.3. Dynamics of sulfite over the course of incubation

The fluorescent probe CY was used to monitor the concentrations of sulfite derived from DHPS metabolism. DHPS and other coexistent ions present in the medium had no visible effect on the fluorescence intensity of the mixture (Fig. S6A). In presence of samples derived from the different growth phases of *R. pomeroyi* DSS-3, *D. shibae* DFL 12 and *R. denitrificans* OCh 114, the fluorescence intensity and color of probe CY showed significantly changes. Before the respective exponential phase of these strains, the reaction of samples with probe made the fluorescence intensity of CY gradually decreased, as well the fading of color (Fig. 3), indicating that these strains produced and excreted sulfite extracellularly. After the exponential phase of these three strains, the extracellular

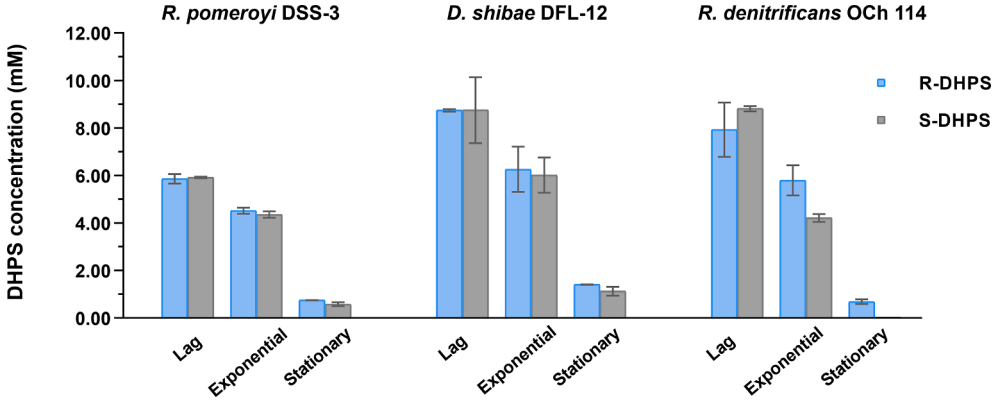

Fig. 2. Concentrations of DHPS remaining in the supernatant during the incubation of *Roseobacter* strains at different growth phases. Error bars represent the standard deviation of triplicate cultures.

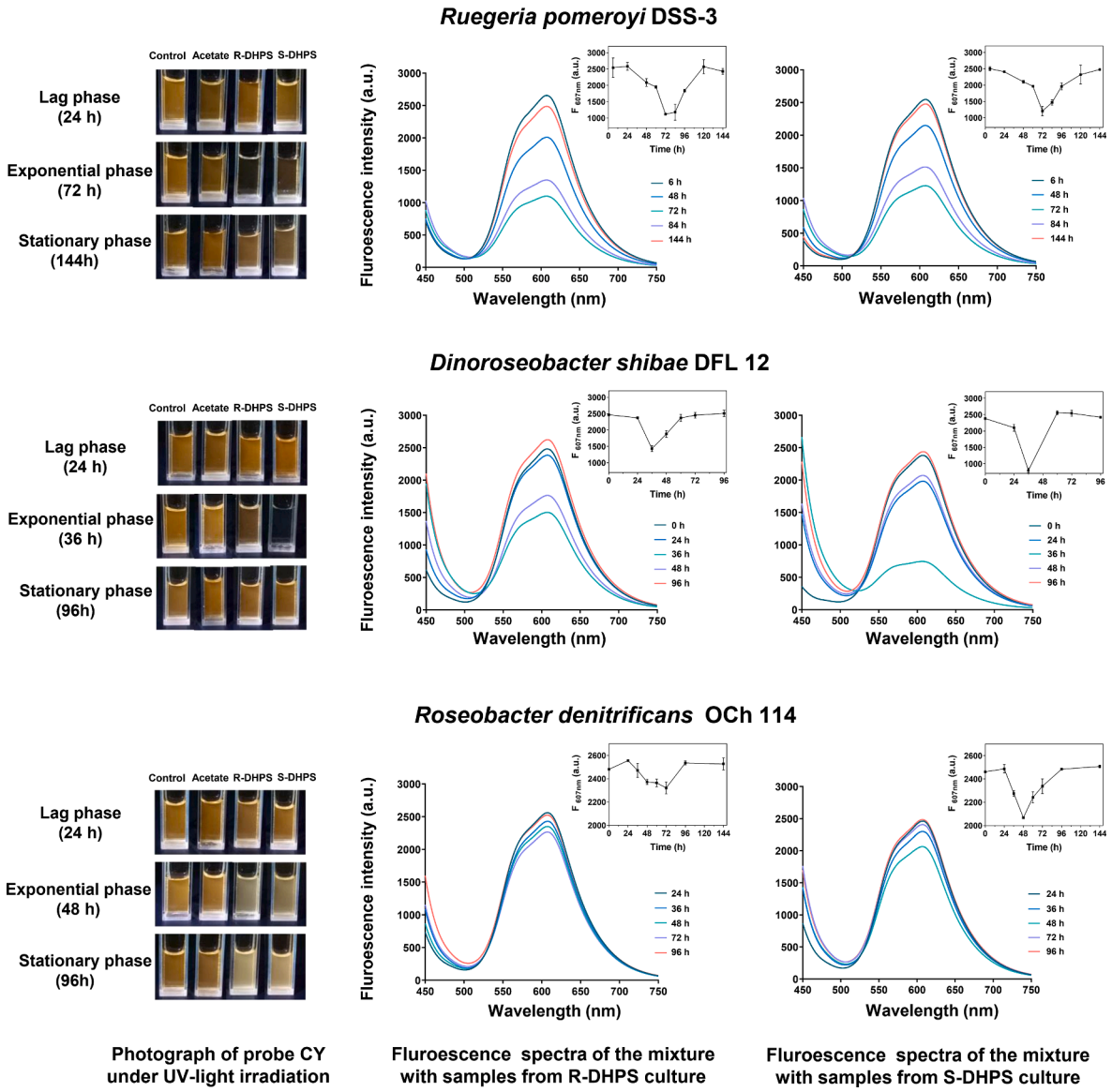

Fig. 3. Detection of sulfite concentration derived from DHPS metabolism. The corresponding samples (5% volume ratio) collected from different culture systems in PBS buffer (pH 7.4, $\lambda_{ex} = 410$ nm) were added to CY (1 μM). Left shows photograph of the CY probe under UV-light irradiation with samples collected at the different growth phases, with the relevant culture mediums shown at the top of pictures. Right shows the fluorescence spectra of CY that reacted with samples taken at different growth phases for different strains grown with R/S-DHPS. The insert curves are time-dependent fluorescence intensity observed for CY ($\lambda_{em} = 607$ nm). Error bars represent the standard deviation of triplicate cultures.

sulfite decreased gradually, indicated by the increasing fluorescence intensity of probe CY as well as the recovering color to yellow (Fig. 3). An additional experiment showed that the extracellular concentration of sulfite decreased with the presence of strain *R. pomeroyi* DSS-3, while sulfite concentration in sterile controls changed by only a negligible amount (Fig. S6B), suggesting that the released sulfite could be further consumed by *R. pomeroyi* DSS-3, as well as by *D. shibae* DFL 12 and *R. denitrificans* OCh 114. While no changes in fluorescence intensity of probe CY were observed when present with samples derived from the culture of *N. italica* DSM 26436 (data not shown), consistent with its failure to utilize DHPS for growth.

3.4. Comparative proteomic analysis of Roseobacter strains

Label-free analysis of total proteins from crude extracts of DHPS- and acetate-grown cells, as well as the different growth phases of DHPS-grown cells, was performed on strains *R. pomeroyi* DSS-3, *D. shibae* DFL 12 and *R. denitrificans* OCh 114. With FDR < 0.01 as the significance threshold and fold-change > 5 or < 0.2 as differential abundance threshold, 194, 191, and 121 proteins were found to be differentially expressed between DHPS- and acetate-grown cells, in strains *R. pomeroyi* DSS-3, *D. shibae* DFL 12, and *R. denitrificans* OCh 114, respectively (Table S1). While 45, 41, and 20 proteins differentially expressed between the different growth phases present in *R. pomeroyi* DSS-3, *D. shibae* DFL 12 and *R. denitrificans* OCh 114, respectively (Table S1).

In all three strains, compared to acetate-grown cells, proteins involved in DHPS metabolism (DHPS transporters, DHPS dehydrogenases, DHPS desulfonation enzymes and sulfite-oxidizing enzymes) were significantly upregulated, while proteins involved in sulfate assimilation were downregulated. Comparative analysis is shown by the heatmap in Fig. 4.

3.4.1. DHPS transporters

DHPS is impermeable to bacterial cytoplasmic membranes unless a transporter is present, with HpsK, HpsL and HpsM as the major transporters of DHPS (Landa et al., 2017). The comparison of DHPS cultured

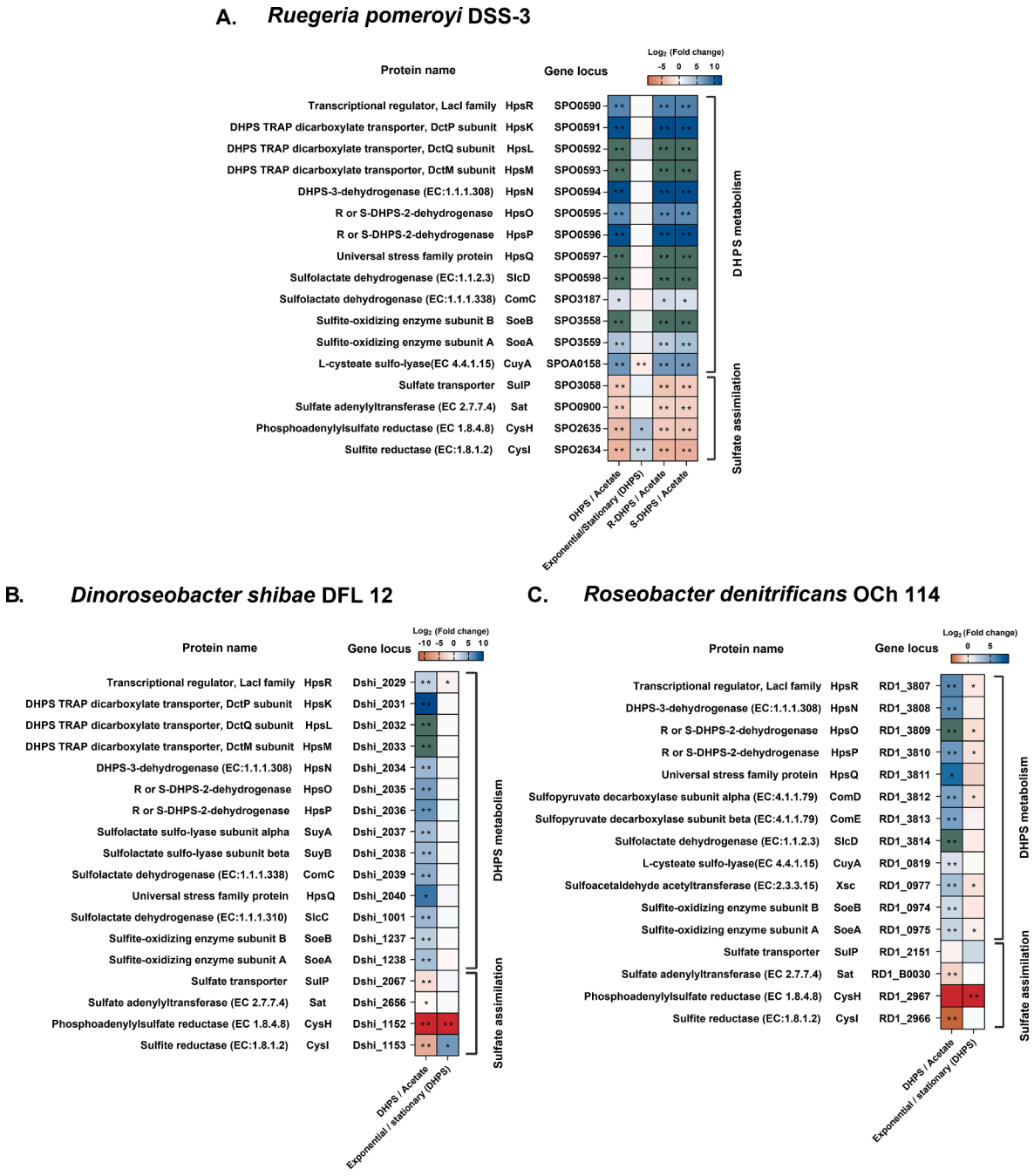

Fig. 4. Comparative proteomic analysis of proteins involved in DHPS metabolism and sulfate assimilation between different groups. Above each heatmap: Log_2 (Fold change) color code. Blue indicates upregulated while orange indicates downregulated protein expression. The comparison patterns between different treatment groups are listed below the respective column. Green indicates proteins observed only in the former groups, red indicates the proteins observed only in the latter groups. "Stationary" indicates samples collected during stationary phase growth in mixed DHPS (R-DHPS: S-DHPS = 1: 1), while all others were collected during exponential phase. "DHPS," cells grown with mixed DHPS, while "R-DHPS" or "S-DHPS" indicates cells grown with pure R-DHPS or S-DHPS, respectively. "Acetate" indicates cells grown with acetate. Since each treatment was performed in triplicate, results are shown as average values. Corrected *P*-values (*q* values) were calculated based on Multiple *t*-test using FDR approach (1%). Significance: *, $q < 0.05$; **, $q < 0.01$.

and acetate cultured cells showed that HpsKLM were responsible for DHPS transport in strains *R. pomeroyi* DSS-3 and *D. shibae* DFL 12, whose expression was upregulated by DHPS (Fig. 4A; Fig. 4B). TRAP dicarboxylate transporters (encoded by RD1_3992 and RD1_3994) were present at a significantly higher abundance in DHPS-grown cells than acetate-grown cells (Table S2), indicating their potential role as DHPS transporters in *R. denitrificans* OCh 114. In additional to strain OCh 114, some organisms lacking homologous *hpsKLM* genes could also grow with DHPS (Mayer et al., 2010), this suggests that otherwise unknown DHPS transporters may exist within DHPS-degraders, indicating the diversity of DHPS transporter system.

3.4.2. DHPS dehydrogenases

In all three strains, significantly upregulated abundances of hydrogenases HpsOPN, as well as the regulators HpsR and HpsQ, were observed in the presence of DHPS as compared to acetate (Fig. 4). The expression of dehydrogenases HpsOP should have been upregulated by S-DHPS compared to R-DHPS, for the conversation of S-DHPS into R-

DHPS (Fig. 1A), however, this was not the case Table S2. Located in the same operon, *hpsNOP* were co-regulated by the same regulator. Both R- and S-DHPS could trigger the expression of the regulator and these hydrogenases simultaneously, thus, no difference in their expression level was found for *R. pomeroyi* DSS-3 between R- and S-DHPS cultures (Table S2).

3.4.3. DHPS desulfonation enzymes

Different strains used distinct enzymes for DHPS desulfonation with the corresponding proteins upregulated in DHPS-grown cells compared

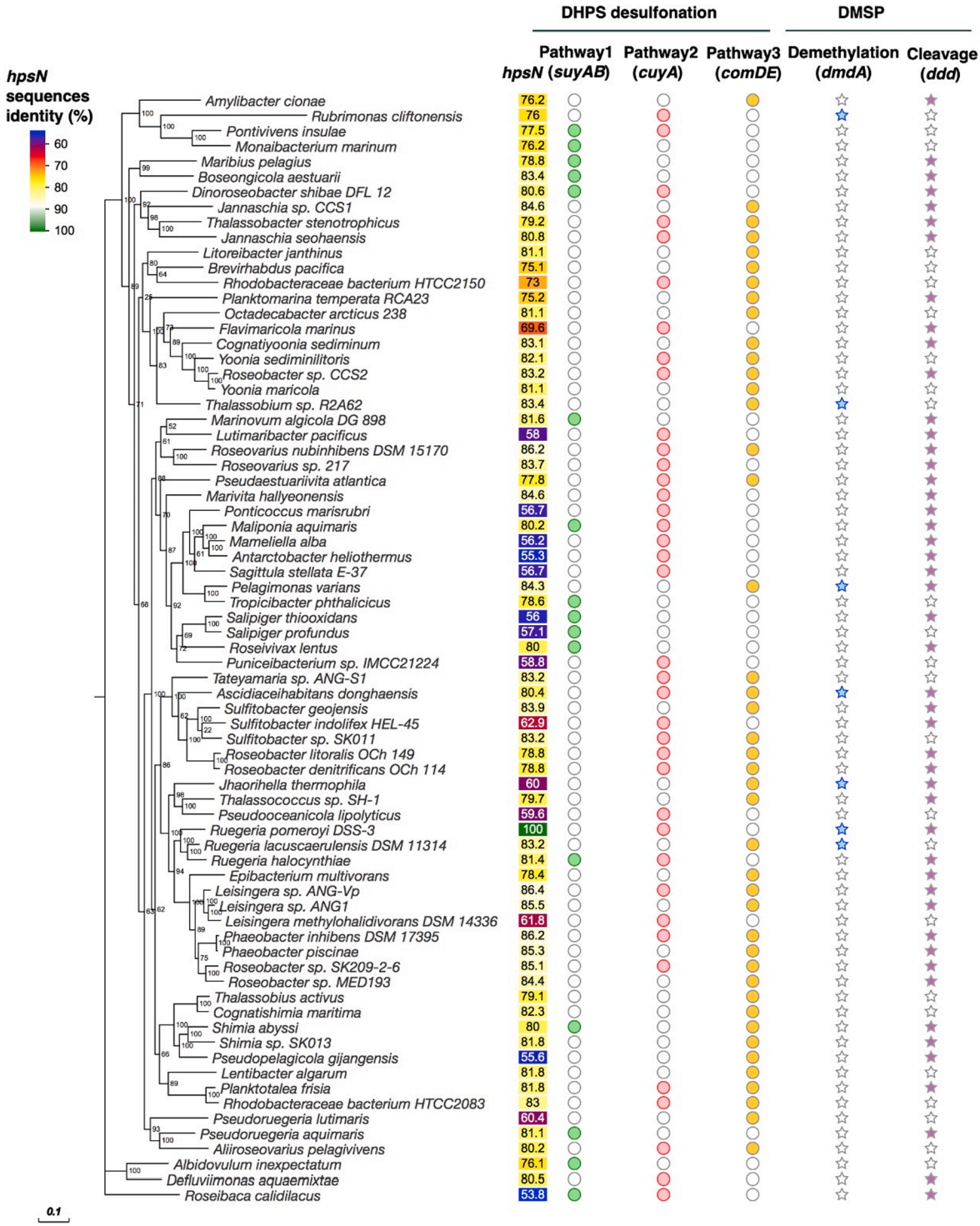

Fig. 5. Diversity of DHPS metabolic genes in *Roseobacter* clade. Organisms within *Roseobacter* clade that possess *hpsN* paralogs, as well as key enzymes involved in DHPS desulfonation, were analyzed. Their genetic potential to catabolize DMSP, via either demethylation (*dmdA*) or cleavage pathway (*ddd*), are shown. The gene cluster information for *Roseobacter* is listed on the right. Bootstrap values are shown on the branches of the phylogenetic tree. The scale bar represents 10% sequence divergence. The identity scores (> 50%) of *hpsN* sequences compared to that of *R. pomeroyi* DSS-3 (SPO0954) are presented with the color code, shown on the upper left. The value near each internal branch is the posterior probability, and the scale bar indicates the number of substitutions per site. Colored, filled circles and stars indicate the presence of the indicated protein-encoding gene. *CuyA*, L-cysteate sulfo-lyase; *suyAB*, sulfolactate sulfo-lyase; *comDE*, sulfopyruvate decarboxylase.

to acetate-grown cells. Proteomic analysis showed that both strains *R. pomeroyi* DSS-3 and *R. denitrificans* OCh 114 desulfonated DHPS via CuyA, while ComDE and Xsc also operated in *R. denitrificans* OCh 114 (Fig. 4A and 4C). *D. shibae* DFL 12 appeared to desulfonate DHPS mainly via SuyAB, with downregulation of CuyA but upregulation of SuyAB in the presence of DHPS (Fig. 4B), indicating that *D. shibae* DFL 12 has a preference for DHPS desulfonation via SuyAB, which might be more favorable for bacterial growth in comparison to using both desulfonation pathways simultaneously.

3.4.4. Sulfite-oxidizing enzymes

The released sulfite from DHPS desulfonation was further consumed by the *Roseobacter* strains themselves. In all strains, the abundance of sulfite-oxidizing enzyme subunits (SoeAB) was much higher in DHPS-grown cells than acetate-grown cells (Fig. 4), indicating that these bacteria could oxidize the sulfite derived from DHPS metabolism. Generally, more than 55% of the sulfur-moiety of DHPS could be recovered in the form of sulfate during bacterial incubations (Mayer et al., 2010), suggesting that the yielded sulfite was mainly used for energy metabolism.

3.4.5. Sulfate assimilation enzymes

In comparison with acetate-grown cells, proteins involved in sulfate assimilation, a pathway for biosynthesis of sulfur-containing amino acids, were observed to be significantly downregulated in the presence of DHPS, including sulfate transporter, sulfate adnylyltransferase, phosphoadenylylsulfate reductase and sulfite reductase (Fig. 4). Lower protein abundances were found during stationary phase than exponential phase, especially for phosphoadenylylsulfate reductase (CysH) and sulfite reductase (CysI) (Fig. 4), the enzymes that converts 3-phosphoadenylyl sulfate to sulfite and reduces sulfite to hydrogen sulfide, respectively (Tang, 2020), suggesting a higher concentration of supplementary reduced sulfur present intracellularly at stationary phase than exponential phase. This proteomic data revealed that DHPS metabolism could supply sufficient amounts of sulfite, as the intermediate for sulfate assimilation. Similarly, marine SAR11 clade lacks a sulfate assimilation pathway (Tripp et al., 2008), but they could use DHPS as an exogenous source of reduced sulfur for growth (Durham et al., 2019).

3.5. Diversity of DHPS catabolism in the Roseobacter clade

A survey of metabolic pathways for DHPS catabolism in 73 *Roseobacter* isolate genomes was performed. The majority of *Roseobacter* bacteria harbored one of the three desulfonation pathways (49 of 73 genomes), while the remaining (24 of 73 genomes) harbored two, with the *comDE* and *cuyA* pathways more common (Fig. 5). Furthermore, species affiliated with the same genus may possess distinct DHPS

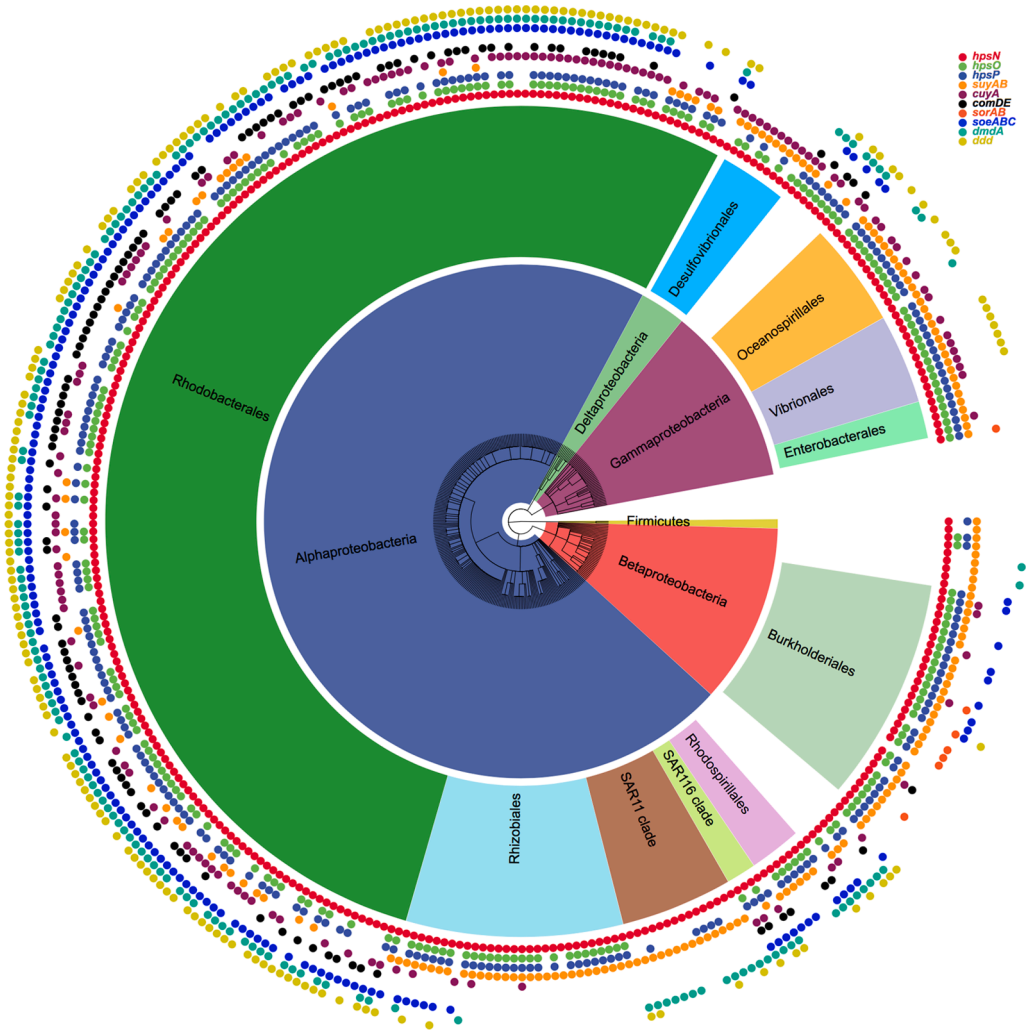

Fig. 6. Distribution of DHPS metabolic genes in publicly available bacterial genomes. The phylogenetic tree was constructed with bacterial 16S rRNA. The genetic potential to degrade DMSP are also shown. Colored circles indicate the presence of the relevant sequences in those genomes (details are available in Table S2), and different colors represent the various genes, as shown in the figure key. Clades with representatives are labelled in different background colors.

desulfonation pathways (Fig. 5), indicating a high variation of DHPS metabolism within *Roseobacter*. More than 90% of the potential DHPS-degraders within *Roseobacter* also exhibit the genetic capacity to degrade DMSP (67 of 73 genomes), via a demethylation pathway that produces methanethiol or/and the cleavage pathway yielding dimethyl sulfide (Moran et al., 2012) (Fig. 5).

We further assessed the metabolic potential of DHPS in other bacteria based on genomic analysis. Genes involved in DHPS metabolism were found to be ubiquitously distributed among a variety of bacterial taxa, more than 73% of whom inhabit marine systems (246/335) (Fig. 6; Table S3). *Alphaproteobacteria* contributed the vast majority of the *hpsN* gene pool (245/335), and were mainly composed of the genus *Roseobacter* (182/245), the order Rhizobiales (29/245), the SAR11 and SAR116 clades (15/245), and the order Rhodospirillales (7/245) (Table S3). The SAR11 clade appears to primarily catabolize DHPS via the *suyAB* pathway, while the *Rhodobacterales*, SAR116, *Rhizobacterales*, and Rhodospirillales groups possess an additional *comDE* or *cuyA* pathway (Table S3), showing a diverse desulfonation pathways within bacteria. The genetic capability for DHPS degradation was also identified in the bacterial orders Burkholderiales, Oceanospirillales, Vibrionales, Enterobacterales, and Desulfovibrionales as well as in the phylum Firmicutes (Fig. 6; Table S3). Meanwhile, the *soeABC* gene cluster was identified in the majority of the *Roseobacter* clade (168/182), all SAR116, and some *Gammaproteobacteria* strains (Table S3). Members of Burkholderiales lack *soeABC* but did possess another sulfite-oxidizing enzyme gene, *sorAB* (Kappler et al., 2000). The sulfite derived from DHPS may be energy source for these sulfite-oxidizing bacteria. Additionally, the majority of the *Alphaproteobacteria* (206/245), as well as some *Gammaproteobacteria* (24/40), possess the genetic potential to degrade DMSP (Fig. 6; Table S2), suggesting that the majority of DHPS degraders are also capable of DMSP utilization, enabling them to inhabit a wide range of ecological niches.

Laboratory incubation experiments showed that *R. pomeroyi* DSS-3 grew with DHPS at a specific growth rate of 1.019 ± 0.00 day^{-1}, which is higher than that of growth with DMSP (0.914 ± 0.17 day^{-1}; $p = 0.48$, *t*-test) and acetate (0.422 ± 0.05 day^{-1}; $p < 0.01$, *t*-test), even though it was supplied with an equivalent amount of carbon (Table S4). DHPS could also support a higher cell yields than DMSP or acetate, as shown by the observed maximum turbidity of OD_{600} (0.225 ± 0.00, 0.103 ± 0.01, and 0.145 ± 0.03 for DHPS, DMSP and acetate, respectively; Table S4). These observations demonstrated that part of the carbon of DMSP would be lost from cells in the form of volatile dimethylsulfide. Furthermore, the presence of other labile organic compounds (such as acetate) could facilitate bacterial growth in DHPS, showing a synergistic effect (Fig. S7; Table S4). Additionally, an incubation experiment was conducted with *in situ* coastal bacterial community, wherein the relative abundance of *Roseobacter* clade increased along with the consumption of DHPS, suggesting they were the DHPS-degraders in this marine ecosystem (Fig. S8). Considered together, the abundant DHPS could be readily metabolized by marine bacteria for growth, producing sulfite which is finally oxidized into sulfate.

4. Conclusions

Genomic and proteomic data showed that *Roseobacter* catabolize R- and S-DHPS by the integration of specific dehydrogenases and desulfonation enzymes, yielding sulfite. Differences were exhibited between *Rosoebacter* strains in the method of desulfonation, through the use of either a single or multiple pathways. The sulfite could be either further oxidized for energy by sulfite-oxidizing enzymes or incorporated into intermediates of sulfate assimilation, as suggested by fluorescent observation and proteomic data. No significant differences in the growth rate and the DHPS consumption rate were observed in *R. pomeroyi* DSS-3 between R- and S-DHPS cultures, consistent with that few proteins expressed differentially. An incubation experiment using a natural marine bacterial community revealed that *Roseobacter* acted as DHPS transformers in the marine environment. Given the ubiquitous genetic capability for DHPS metabolism in *Roseobacter* and other bacteria, DHPS serves as an energy and biosynthesis resource instead of source of toxic sulfide, thus having no negative impacts on the health of marine organisms.

CRediT authorship contribution statement

Xiaofeng Chen: Investigation, Methodology, Formal analysis, Writing – original draft, Writing – review & editing. **Le Liu:** Writing – review & editing. **Xiang Gao:** Methodology, Writing – review & editing. **Xi Dai:** Methodology, Writing – review & editing. **Yu Han:** Methodology, Writing – review & editing. **Quanrui Chen:** Writing – review & editing. **Kai Tang:** Project administration, Formal analysis, Writing – review & editing, Supervision.

Declaration of Competing Interest

The authors declare that they have no known competing financial interests or personal relationships that could have appeared to influence the work reported in this paper.

Acknowledgments

This study was supported by the National Key Research and Development Program of China (2020YFA0608300), the National Natural Science Foundation of China project (41776167, 42076160, 91751207). We are also grateful to Dr. James Walter Voordeckers for language polishing of the manuscript.

Appendix A. Supplementary material

Supplementary data to this article can be found online at https://doi.org/10.1016/j.envint.2021.106829.

References

Altschul, S.F., Madden, T.L., Schäffer, A.A., Zhang, J., Zhang, Z., Miller, W., Lipman, D.J., 1997. Gapped BLAST and PSI-BLAST: a new generation of protein database search programs. Nucleic Acids Res. 25, 3389–3402.

Biebl, H., Allgaier, M., Tindall, B.J., Koblizek, M., Lünsdorf, H., Pukall, R., Wagner-Döbler, I., 2005. *Dinoroseobacter shibae* gen. nov., sp. nov., a new aerobic phototrophic bacterium isolated from dinoflagellates. Int. J. Syst. Evol. Microbiol. 55, 1089–1096.

Carbonero, F., Benefiel, A.C., Alizadeh-Ghamsari, A.H., Gaskins, H.R., 2012. Microbial pathways in colonic sulfur metabolism and links with health and disease. Front. Physiol. 3, 448.

Cox, J., Mann, M., 2008. MaxQuant enables high peptide identification rates, individualized p.p.b.-range mass accuracies and proteome-wide protein quantification. Nat. Biotechnol. 26, 1367–1372.

Dahl, C., Franz, B., Hensen, D., Kesselheim, A., Zigann, R., 2013. Sulfite oxidation in the purple sulfur bacterium *Allochromatium vinosum*: identification of SoeABC as a major player and relevance of SoxYZ in the process. Microbiology (Reading) 159, 2626–2638.

Denger, K., Smits, T.H., Cook, A.M., 2006. L-cysteate sulpho-lyase, a widespread pyridoxal 5'-phosphate-coupled desulphonative enzyme purified from *Silicibacter pomeroyi* DSS-3^T. Biochem. J. 394, 657–664.

Denger, K., Weiss, M., Felux, A.-K., Schneider, A., Mayer, C., Spiteller, D., Huhn, T., Cook, A.M., Schleheck, D., 2014. Sulphoglycolysis in *Escherichia coli* K-12 closes a gap in the biogeochemical sulphur cycle. Nature 507, 114.

Durham, B.P., Boysen, A.K., Carlson, L.T., Groussman, R.D., Heal, K.R., Cain, K.R., Morales, R.L., Coesel, S.N., Morris, R.M., Ingalls, A.E., Armbrust, E.V., 2019. Sulfonate-based networks between eukaryotic phytoplankton and heterotrophic bacteria in the surface ocean. Nat. Microbiol. 4, 1706–1715.

Durham, B.P., Sharma, S., Luo, H., Smith, C.B., Amin, S.A., Bender, S.J., Dearth, S.P., Van Mooy, B.A., Campagna, S.R., Kujawinski, E.B., Armbrust, E.V., Moran, M.A., 2015. Cryptic carbon and sulfur cycling between surface ocean plankton. Proc. Natl. Acad. Sci. USA 112, 453–457.

Durham, B.P., Dearth, S.P., Sharma, S., Amin, S.A., Smith, C.B., Campagna, S.R., Armbrust, E.V., Moran, M.A., 2017. Recognition cascade and metabolite transfer in a marine bacteria-phytoplankton model system. Environ. Microbiol. 19, 3500–3513.

Gonzalez, J.M., Covert, J.S., Whitman, W.B., Henriksen, J.R., Mayer, F., Scharf, B., Schmitt, R., Buchan, A., Fuhrman, J.A., Kiene, R.P., Moran, M.A., 2003. *Silicibacter pomeroyi* sp. nov. and Roseovarius nubinhibens sp. nov.,

dimethylsulfoniopropionate-demethylating bacteria from marine environments. Int. J. Syst. Evol. Microbiol. 53, 1261–1269.
Harwood, J.L., Nicholls, R.G., 1979. The plant sulpholipid – a major component of the sulphur cycle. Biochem. Soc. Trans. 7, 440–447.
Kappler, U., Bennett, B., Rethmeier, J., Schwarz, G., Deutzmann, R., McEwan, A.G., Dahl, C., 2000. Sulfite: Cytochrome c oxidoreductase from *Thiobacillus novellus*. Purification, characterization, and molecular biology of a heterodimeric member of the sulfite oxidase family. J. Biol. Chem. 275, 13202–13212.
Landa, M., Burns, A.S., Durham, B.P., Esson, K., Nowinski, B., Sharma, S., Vorobev, A., Nielsen, T., Kiene, R.P., Moran, M.A., 2019. Sulfur metabolites that facilitate oceanic phytoplankton-bacteria carbon flux. ISME J. 13, 2536–2550.
Landa, M., Burns, A.S., Roth, S.J., Moran, M.A., 2017. Bacterial transcriptome remodeling during sequential co-culture with a marine dinoflagellate and diatom. ISME J. 11, 2677–2690.
Liu, J., Wei, Y., Lin, L., Teng, L., Yin, J., Lu, Q., Chen, J., Zheng, Y., Li, Y., Xu, R., Zhai, W., Liu, Y., Liu, Y., Cao, P., Ang, E.L., Zhao, H., Yuchi, Z., Zhang, Y., 2020. Two radical-dependent mechanisms for anaerobic degradation of the globally abundant organosulfur compound dihydroxypropanesulfonate. Proc. Natl. Acad. Sci. USA 117, 15599–15608.
Mayer, J., Huhn, T., Habeck, M., Denger, K., Hollemeyer, K., Cook, A.M., 2010. 2,3-Dihydroxypropane-1-sulfonate degraded by *Cupriavidus pinatubonensis* JMP134: purification of dihydroxypropanesulfonate 3-dehydrogenase. Microbiology (Reading) 156, 1556–1564.
Moran, M.A., Durham, B.P., 2019. Sulfur metabolites in the pelagic ocean. Nat. Rev. Microbiol. 17, 665–678.
Moran, M.A., Reisch, C.R., Kiene, R.P., Whitman, W.B., 2012. Genomic insights into bacterial DMSP transformations. Ann. Rev. Mar. Sci. 4, 523–542.
Nelson, D.M., Treguer, P., Brzezinski, M.A., Leynaert, A., Queguiner, B., 1995. Production and dissolution of biogenic silica in the ocean: Revised global estimates, comparison with regional data and relationship to biogenic sedimentation. Global Biogeochem. Cy. 9, 359–372.
Ng, S.C., Shi, H.Y., Hamidi, N., Underwood, F.E., Tang, W., Benchimol, E.I., Panaccione, R., Ghosh, S., Wu, J.C.Y., Chan, F.K.L., Sung, J.J.Y., Kaplan, G.G., 2017. Worldwide incidence and prevalence of inflammatory bowel disease in the 21st century: a systematic review of population-based studies. Lancet. 390, 2769–2778.
Nie, J., Sun, H., Zhao, Y., Dai, X., Ni, Z., 2020. An efficient hemicyanine dyes-based ratiometric fluorescence probe for sulfur dioxide derivatives in live-cells and seawater. Spectrochim. Acta. A: Mol. Biomol. Spectrosc. 247, 119128.
Shiba, T., 1991. *Roseobacter litoralis* gen. nov., sp. nov., and *Roseobacter denitrificans* sp. nov., aerobic pink-pigmented bacteria which contain bacteriochlorophyll a. Syst. Appl. Microbiol. 14, 140–145.
Sohn, H.Y., Murray, D.B., Kuriyama, H., 2000. Ultradian oscillation of *Saccharomyces cerevisiae* during aerobic continuous culture: hydrogen sulphide mediates population synchrony. Yeast 16 (13), 1185–1190.
Stamatakis, A., 2014. RAxML version 8: a tool for phylogenetic analysis and post-analysis of large phylogenies. Bioinformatics 30, 1312–1313.
Tamura, K., Stecher, G., Peterson, D., Filipski, A., Kumar, S., 2013. MEGA6: Molecular evolutionary genetics analysis version 6.0. Mol. Biol. Evol. 30, 2725–2729.
Tang, K., 2020. Chemical diversity and biochemical transformation of biogenic organic sulfur in the ocean. Front. Mar. Sci. 7.
Tripp, H.J., Kitner, J.B., Schwalbach, M.S., Dacey, J.W.H., Wilhelm, L.J., Giovannoni, S. J., 2008. SAR11 marine bacteria require exogenous reduced sulphur for growth. Nature 452, 741–744.
Tyanova, S., Temu, T., Sinitcyn, P., Carlson, A., Hein, M.Y., Geiger, T., Mann, M., Cox, J., 2016. The Perseus computational platform for comprehensive analysis of (prote) omics data. Nat. Methods 13, 731–740.
Vandecandelaere, I., Nercessian, O., Segaert, E., Achouak, W., Mollica, A., Faimali, M., Vandamme, P., 2009. *Nautella italica* gen. nov., sp. nov., isolated from a marine electroactive biofilm. Int. J. Syst. Evol. Microbiol. 59, 811–817.
Wang, R., Zhang, Z., Sun, J., Jiao, N., 2020. Differences in bioavailability of canonical and non-canonical D-amino acids for marine microbes. Sci. Total. Environ. 733, 139216.